Inorganic Chemistry

Article

pubs.acs.org/IC

On Why the Two Polymorphs of $NaFePO_4$ Exhibit Widely Different Magnetic Structures: Density Functional Analysis

Hee Hwan Kim,[†] Il Han Yu,[†] Hoon Sik Kim,[†] Hyun-Joo Koo,*[,†] and Myung-Hwan Whangbo*[,‡]

[†]Department of Chemistry and Research Institute for Basic Science, Kyung Hee University, Seoul 130-701, Republic of Korea

[‡]Department of Chemistry, North Carolina State University, Raleigh, North Carolina 27695-8204, United States

Supporting Information

ABSTRACT: Triphylite-$NaFePO_4$ is a cathode material for Na^+-ion batteries, whereas its alternative polymorph maricite-$NaFePO_4$ is not. These two different polymorphs exhibit widely different magnetic structures; the ordered magnetic structure of triphylite-$NaFePO_4$ below ~50 K is described by the propagation vector $q_1 = (0, 0, 0)$ with collinear spins, and that of maricite-$NaFePO_4$ below ~13 K is described by $q_2 = (1/2, 0, 1/2)$ with noncollinear spins. We probed the causes for these differences by calculating the spin exchange interactions of the two polymorphs and determining the preferred orientations of their high-spin Fe^{2+} (d^6, $S = 2$) ions on the basis of density functional calculations. Our study shows that maricite-$NaFePO_4$ is not spin-frustrated, which is also the case for triphylite-$NaFePO_4$, that the ordered magnetic structure of triphylite-$NaFePO_4$ is determined mainly by spin exchange, whereas that of maricite-$NaFePO_4$ is determined by both spin exchange and magnetic anisotropy, and that the preferred spin orientations in the two polymorphs can be explained by perturbation theory using spin−orbit coupling as the perturbation.

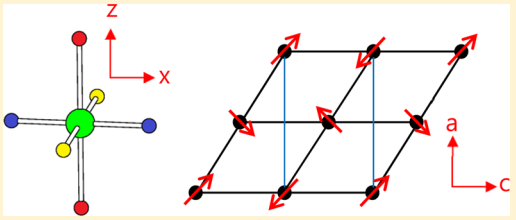

1. INTRODUCTION

$NaFePO_4$ is important as a cathode material for Na^+-ion batteries and has two distinct polymorphs, triphylite-$NaFePO_4$ and maricite-$NaFePO_4$ (hereafter referred to as t-$NaFePO_4$ and m-$NaFePO_4$, respectively, for simplicity).[1−3] Both polymorphs are made up of distorted FeO_6 octahedra containing high-spin Fe^{2+} (d^6, $S = 2$) and distorted PO_4 tetrahedra. In t-$NaFePO_4$, the FeO_6 octahedra are corner-shared to form two-dimensional (2D) layers parallel to the *bc*-plane (Figure 1a), and these 2D layers are linked by PO_4 tetrahedra such that one-dimensional (1D) channels are present through which Na^+ cations can diffuse (Figure 1b). t-$NaFePO_4$ can deliver a reversible discharge exceeding 120 mAh/g with Fe^{3+}/Fe^{2+} redox activity around 3 V.[4,5] In contrast, m-$NaFePO_4$ has edge-sharing FeO_6 octahedra to form chains along the *b*-axis (Figure 2a), and these chains are linked by PO_4 tetrahedra to form a three-dimensional (3D) crystal structure with no Na^+-ion diffusion channel. Thus, Na^+ ions are electrochemically inactive in m-$NaFePO_4$,[6] which is thermodynamically more stable than t-$NaFePO_4$.[1]

The magnetic properties of t- and m-$NaFePO_4$ probed by magnetic susceptibility (χ), neutron powder diffraction (NPD) and specific heat measurements[3] present seemingly puzzling features. The Curie−Weiss temperatures θ of t- and m-$NaFePO_4$ are similar (−84 and −83 K, respectively) and indicate the presence of dominant antiferromagnetic (AFM) interactions in both polymorphs. Specific heat measurements reveal that a long-range AFM ordering takes place at $T_N \approx 50$ and 13 K for t- and m-$NaFePO_4$, respectively.[3] In general, a magnetic system is regarded as spin-frustrated [7] when its frustration index $f = |\theta|/T_N$ is equal to 6 or greater. In such a

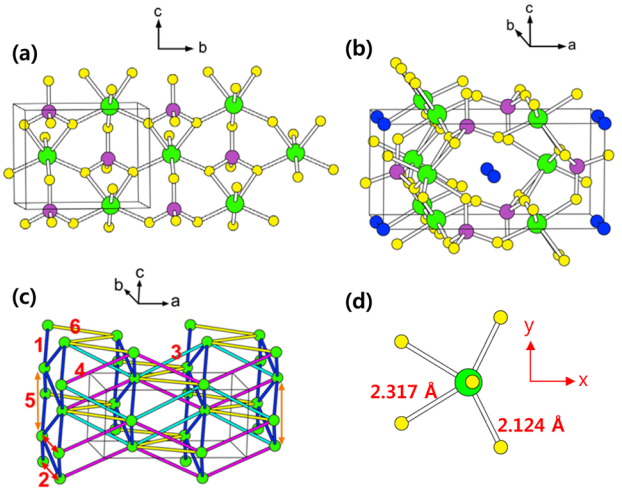

Figure 1. Crystal structure and spin exchange paths of t-$NaFePO_4$. (a) A projection view of an isolated $FePO_4$ layer (green circle = Fe, purple circle = P, yellow circle = O) with PO_4 units attached above and below. (b) A perspective view of the crystal structure (blue circle = Na). (c) Spin exchange paths of t-$NaFePO_4$ defined using only the Fe atoms, where the numbers 1−6 represent the spin exchange paths J_1−J_6, respectively. (d) An isolated FeO_6 unit with the Cartesian coordinate system employed to describe its d-states. The length of the Fe−O along the *z*-axis is 2.054 Å.

Received: March 13, 2015
Published: April 30, 2015

DOI: 10.1021/acs.inorgchem.5b00577
Inorg. Chem. 2015, 54, 4966−4971

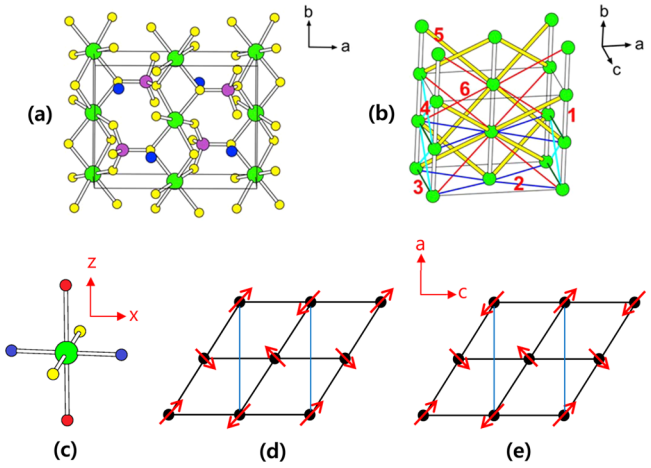

Figure 2. Crystal structure, spin exchange paths, and magnetic structure of m-$NaFePO_4$. (a) A perspective view of the crystal structure (green circle = Fe, purple circle = P, yellow circle = O, blue circle = Na). (b) Spin exchange paths of m-$NaFePO_4$ defined using only the Fe atoms, where the numbers 1−6 represent the spin exchange paths J_1−J_6, respectively. (c) An isolated FeO_6 unit with the Cartesian coordinate system employed to describe its d-states, where the short Fe−O_s, the medium Fe−O_m and the long Fe−O_l bonds are indicated by blue, yellow, and red O atoms, respectively. (d) An arrangement of orthogonal spins leading to doubling of the *a*-axis length, and (e) leading to no *a*-axis doubling. The rectangles in (d) and (e) represent the magnetic unit cell.

magnetic system, attainment of a 3D AFM order is expected to be difficult and may involve a complex magnetic structure.[7] Thus, it is surprising that m-$NaFePO_4$ undergoes a 3D AFM ordering at 13 K despite its frustration index being greater than 6 (~6.3). Nevertheless, unlike the case of t-$NaFePO_4$, for which $f \approx 1.7$, the $1/\chi$ vs T plot for m-$NaFePO_4$ is quite nonlinear above T_N such that its Curie−Weiss temperature (−83 K), estimated using the linear portion of the plot, may not be accurate because the linear region is very narrow (namely, 240−300 K). The latter can be tested by estimating the Curie−Weiss temperatures of t- and m-$NaFePO_4$ on the basis of mean-field theory[8] once their spin exchange parameters are known. Another puzzling feature of the two polymorphs is the sharp difference between their ordered magnetic structures. The NPD measurements show that the ordered magnetic structure of t-$NaFePO_4$ is described by the propagation vector $q_1 = (0, 0, 0)$ with collinear spins (parallel to the *b*-direction), but that of m-$NaFePO_4$ is $q_2 = (1/2, 0, 1/2)$ with noncollinear spins. In the latter, spins parallel approximately to the (*a*+*c*)-direction form chains along the *c*-direction, as do spins approximately parallel to the (−*a*+*c*)-direction, and these chains alternate along the *a*-direction.[3] In general, a magnetic system adopts a noncollinear spin order when its spin exchanges experience spin frustration (not as strong as in a system with $f \geq 6$). One may wonder how m-$NaFePO_4$ reduces its spin frustration (if there is any) by adopting the particular (1/2, 0, 1/2) magnetic structure. The preferred orientations of spins are a consequence of spin−orbit coupling (SOC), which are primarily local interactions. Recently, it was found that the preferred spin orientations of transition-metal magnetic ions can be accounted for in terms of perturbation theory with SOC as the perturbation and crystal-field split d-states as the unperturbed state.[9−13] It is interesting to see how the observed orientations of the Fe^{2+} spins in t- and m-$NaFePO_4$ are related to the d-states of their FeO_6 octahedra.

To address these issues, we first evaluated the spin exchange interactions of t- and m-$NaFePO_4$ and then determined the preferred orientations of their Fe^{2+} spins on the basis of density functional theory (DFT) calculations. We show that m-$NaFePO_4$ is not spin-frustrated just as in the case of t-$NaFePO_4$, that the ordered magnetic structure of t-$NaFePO_4$ is largely determined by spin exchange, whereas that of m-$NaFePO_4$ is determined by both spin exchange and magnetic anisotropy, and that the preferred orientations of the high-spin Fe^{2+} (d^6, $S = 2$) ions in the two polymorphs can be explained by perturbation theory using SOC as perturbation.

2. EXPERIMENTAL SECTION

We carried out spin-polarized DFT calculations for t- and m-$NaFePO_4$ by employing the projector augmented wave method encoded in the Vienna ab initio simulation package[14−16] with the generalized gradient approximation of Perdew, Burke and Ernzerhof [17] for the exchange-correlation corrections with a plane wave cutoff energy of 480 eV and threshold of self-consistent-field energy convergence of 10^{-6} eV. The irreducible Brillouin zone was sampled with 32 k points. To properly describe the electron correlation associated with the Fe 3d states, the DFT plus on-site repulsion U (DFT+U) [18] method was applied with effective $U_{eff} = U - J = 4$ and 5 eV for t-$NaFePO_4$ and $U_{eff} = U - J = 4$, 5, and 6 eV for m-$NaFePO_4$ on the Fe atom. The preferred spin orientations of t- and m-$NaFePO_4$ were determined by performing DFT+U calculations including SOC (DFT+U+SOC). To simplify our DFT+U+SOC calculations, we replaced all of the Fe^{2+} ions, except for the one selected, of a unit cell with nonmagnetic Zn^{2+} ions and then performed DFT+U+SOC calculations for the Fe^{2+} spin of the selected FeO_6 octahedron as a function of the spin orientation.

3. RESULTS AND DISCUSSION

A. Energy-Mapping Analysis of Spin Exchanges. We considered six spin exchange paths for t-$NaFePO_4$ (Figure 1c) and for m-$NaFePO_4$ (Figure 2b). For both t- and m-$NaFePO_4$, the spin exchange J_1 is an Fe−O−Fe exchange, whereas J_2−J_6 are Fe−O···O−Fe exchanges. The Fe···Fe and O···O distances associated with the spin exchange paths J_1−J_6 are summarized in Table 1. To evaluate these spin exchanges, we employed the seven ordered spin states shown in Figures S1 and S2 in the Supporting Information for t- and m-$NaFePO_4$, respectively. The relative energies of these ordered spin states obtained from

Table 1. Geometrical Parameters Associated with the Spin Exchange Paths in t-$NaFePO_4$ and m-$NaFePO_4$

t-$NaFePO_4$			
		Fe···Fe (Å)	O···O (Å)
Fe−O−Fe	J_1	4.037[a]	
Fe−O···O−Fe	J_2	6.198	2.386
	J_3	5.817	2.484
	J_4	5.692	2.549
	J_5	4.936	2.585
	J_6	5.398	2.484
m-$NaFePO_4$			
		Fe···Fe (Å)	O···O (Å)
Fe−O−Fe	J_1	3.421[a]	
Fe−O···O−Fe	J_2	5.139	2.503
	J_3	5.028	2.503
	J_4	6.082	2.520
	J_5	6.173	2.504
	J_6	6.173	2.573

[a]∠ Fe−O−Fe = 130.8°. [b]∠ Fe−O−Fe = 93.6°, 101.8°.

DOI: 10.1021/acs.inorgchem.5b00577
Inorg. Chem. 2015, 54, 4966−4971

DFT+U calculations are summarized in Table S1 in the Supporting Information. To extract the values of J_1−J_6 from these electronic structure calculations, we expressed the total spin exchange interaction energies of the ordered spin states in terms of the Heisenberg spin Hamiltonian

$$\hat{H} = -\sum_{i<j} J_{ij}\hat{S}_i\cdot\hat{S}_j \quad (1)$$

where $J_{ij} = J_1$−J_6 is the spin exchange parameters for the spin exchange interactions between the spin sites i and j, and $\hat{S}_i$ and $\hat{S}_j$ are the spin operators at the spin sites i and j, respectively. Then, for each of the spin ordered states of t- and m-$NaFePO_4$, the total spin exchange energy per chemical unit cell (i.e., per 16 formula units (FUs)), can be written as

$$E = (n_1J_1 + n_2J_2 + n_3J_3 + n_4J_4 + n_5J_5 + n_6J_6)(N^2/4) \quad (2)$$

by applying the energy expressions obtained for spin dimers with N unpaired spins per spin site (in the present case, $N = 4$ for the high-spin Fe^{2+} ions).[19,20] The coefficients n_1−n_6 for the spin ordered states of t- and m-$NaFePO_4$ are summarized in Table S2 in the Supporting Information. Then, by mapping the relative energies of the spin ordered states onto the corresponding energies expected from the total spin exchange energies,[21,22] we obtain the values of J_1−J_6 summarized in Table 1.

In the mean-field theory,[8] the Curie−Weiss temperature θ of a magnetic system is related to its spin exchanges as

$$\theta = \frac{S(S+1)}{3k_B}\sum_i z_iJ_i \quad (3)$$

where the summation runs over all nearest neighbors for a given spin site, z_i is the number of nearest neighbors connected by the spin exchange parameter J_i, and S is the spin quantum number of each spin site (i.e., $S = 2$ for high-spin Fe^{2+}). According to the spin exchange paths given in Figures 1c and 2b, the Curie−Weiss temperatures of t- and m-$NaFePO_4$ are related to their spin exchanges as $\theta \approx 4(2J_1 + J_2 + J_3 + J_4 + J_5 + J_6)/k_B$ for t-$NaFePO_4$ and $\theta \approx 4(J_1 + 2J_2 + J_3 + 2J_4 + 2J_5 + 2J_6)/k_B$ for m-$NaFePO_4$. The calculated θ values are summarized in Table 1.

B. Spin Exchange and Magnetic Structure. The three strongest spin exchanges of t-$NaFePO_4$ are J_1, J_6 and J_3, all of which are AFM (Table 1a) with relative strengths of $J_6/J_1 \approx 1/2$ and $J_3/J_1 \approx 1/3$. The J_1 exchange paths form 2D AFM layers parallel to the bc-plane. When these 2D AFM layers are antiferromagnetically coupled by J_6 to form a 3D AFM lattice, (J_1, J_6, J_3) and (J_1, J_6, J_4) exchange triangles occur. Because J_1, J_6, and J_3 are all AFM, each (J_1, J_6, J_3) triangle can lead to some spin frustration. However, J_3 may not add much spin frustration to the 3D AFM lattice because it is weaker than J_1 and J_6. Furthermore, the J_4 exchange is FM and thus strengthens the 3D AFM lattice made up of J_1 and J_6 through the (J_1, J_6, J_4) exchange triangles. The remaining spin exchanges, J_2 and J_5, are weak. Therefore, t-$NaFePO_4$ should have a 3D AFM lattice determined by J_1 and J_6, the unit cell of which is identical to that of the chemical unit cell. This explains the observed magnetic structure $q_1 = (0, 0, 0)$.[3] The Curie−Weiss temperature calculated for t-$NaFePO_4$ using the spin exchange parameters is comparable in magnitude to the experimental value (Table 1a).

In general, m-$NaFePO_4$ has no strong spin exchange, and its strong AFM exchanges are weak compared to those of t-$NaFePO_4$. The Curie−Weiss temperature θ of m-$NaFePO_4$, estimated from the mean-field theory, is smaller than that of t-$NaFePO_4$ by a factor of ∼3.5. This suggests that the experimental θ derived for m-$NaFePO_4$ from the linear portion of the $1/\chi$ vs T plot is overestimated in magnitude by a similar factor. Because the T_N of m-$NaFePO_4$ is ∼4 times smaller than that of t-$NaFePO_4$, the frustration indices f of t- and m-$NaFePO_4$ should be similar.

The Fe−O−Fe exchange J_1 is AFM in t-$NaFePO_4$ but is FM in m-$NaFePO_4$. This difference is related to the fact that the ∠Fe−O−Fe angle is considerably larger for t-$NaFePO_4$ (130.8°) than for m-$NaFePO_4$ (93.6° and 101.8°).[23] In m-$NaFePO_4$ the exchange J_1 forms FM chains parallel to the b-direction (Figure 2b). The magnetic superstructure $q_2 = (1/2, 0, 1/2)$ [3] of m-$NaFePO_4$ means that, in the magnetic structure, the a- and c-axes lengths are doubled with respect to the chemical unit cell, whereas the b-axis length remains the same. Let us first consider the possible spin arrangement along the b- and c-directions. In the bc-plane, the FM chains consisting of J_1 interact through J_3 and J_4. The AFM J_4 is considerably stronger than the FM J_3 such that, in terms of J_1, J_3, and J_4 alone, the FM chains defined by J_1 are antiferromagnetically coupled along the c-direction. This explains the doubling of the c-axis length without changing the b-axis length. The antiferromagnetically coupled FM chains in the layers parallel to the bc-planes (hereafter ∥bc-layers) interact along the a-direction by the "interlayer" exchanges J_5, J_2, and J_6. The exchange J_5 is AFM, is the strongest among J_1−J_6, and leads to spin frustration in the (J_5, J_1, J_4, J_5) spin quadrangles. Because J_1 is the weakest spin exchange among J_1, J_4, and J_5, the spin arrangement of each ∥bc-layer derived solely from J_1, J_3, and J_4 cannot remain valid once the interlayer spin exchanges J_5, J_2, and J_6 are taken into consideration. For the interlayer spin exchanges to exert no effect, the spins of one ∥bc-layer should be nearly perpendicular to those of its adjacent ∥bc-layers, which is precisely what has been observed experimentally.[3]

This consideration for m-$NaFePO_4$ raises a couple of questions. First, it is unclear why the Fe^{2+} ions should adopt such spin orientations. Because the FeO_6 octahedra of m-$NaFePO_4$ have three different sets of Fe−O bonds in the *trans* arrangement (Figure 2c), one might speculate that the magnetic anisotropy of each Fe^{2+} ion (namely, the reference of one spin direction over the other directions at each spin site) is responsible for these spin orientations. Second, if this is true, the magnetic anisotropy must be considerably strong to overcome the effect of the strongest "interlayer" spin exchange J_5 (Table 2). We next address these and other related issues.

C. Preferred Spin Orientation and Magnetic Superstructure. As described in section 2, we carried out DFT+U+SOC calculations for selected FeO_6 octahedra of t- and m-$NaFePO_4$. As depicted in Figure 1d, the FeO_6 octahedra of t-$NaFePO_4$ are severely distorted. With the Cartesian coordinates chosen for a selected FeO_6 octahedron of t-$NaFePO_4$ as in Figure 1d, our DFT+U+SOC calculations showed that the preferred orientation of the Fe^{2+} spin is the y-axis direction (Table 3), which is parallel to the b-direction of t-$NaFePO_4$. This result is in agreement with the observed spin orientation. Note that the magnetic anisotropy of the Fe^{2+} ion favoring the local y-axis spin orientation is slightly stronger than the strongest AFM exchange between the Fe^{2+} ions (7.3−8.8 vs 5.3−6.9 k_BK). The FeO_6 octahedra of m-$NaFePO_4$ are also

DOI: 10.1021/acs.inorgchem.5b00577
Inorg. Chem. 2015, 54, 4966−4971

Table 2. Spin Exchange Parameters J_i/k_B (i = 1−6) (in K) and the Mean-Field-Theory Curie−Weiss Temperature θ (in K) Obtained From DFT+U Calculations for t-$NaFePO_4$ and m-$NaFePO_4$

t-$NaFePO_4$		
	U_{eff} = 4 eV	U_{eff} = 5 eV
J_1/k_B	−6.94	−5.31
J_2/k_B	−0.65	−0.37
J_3/k_B	−2.16	−1.66
J_4/k_B	+1.84	+1.38
J_5/k_B	−0.51	−0.38
J_6/k_B	−3.35	−2.56
θ	−74.9	−56.8
m-$NaFePO_4$		
	U_{eff} = 4 eV	U_{eff} = 5 eV	U_{eff} = 6 eV
J_1/k_B	+1.01	+0.63	+0.40
J_2/k_B	−0.22	−0.16	−0.12
J_3/k_B	+0.18	+0.13	+0.10
J_4/k_B	−1.31	−0.96	−0.69
J_5/k_B	−1.66	−1.22	−0.87
J_6/k_B	−0.12	−0.09	−0.07
θ	−21.8	−16.4	−12.0

Table 3. Relative Energies ΔE (in k_BK/Fe) of various spin orientations of the FeO_6 octahedra in t-$NaFePO_4$ and m-$NaFePO_4$ Obtained From DFT+U+SOC (with U_{eff} = 4eV) Calculations[a]

	x	y	z
t-$NaFePO_4$	8.81	0.00	7.31
m-$NaFePO_4$	0.00	8.70	7.54

[a]For the definition of the coordinate axes, see Figure 1d and 2c for for t-$NaFePO_4$ and m-$NaFePO_4$, respectively.

distorted as depicted in Figure 2c, where each FeO_6 octahedron has three sets of Fe-O bonds (i.e., Fe−O_s = 1.992 Å, Fe−O_m = 2.189 Å, and Fe−O_l = 2.347 Å) in the *trans* arrangement. According to our DFT+U+SOC calculations, the preferred orientation of the Fe^{2+} spin is along the x-axis direction (Table 3), namely, along the short Fe−O_s bond. This finding is in agreement with experimental data. Thus, the reason why the spins of one ||bc-layer are nearly orthogonal to those of its adjacent ||bc-layers lies in the fact that the Fe−O_s bonds in the FeO_6 octahedra of one ||bc-layer are approximately oriented along the (a+c)-direction, wheras those in the FeO_6 octahedra of its adjacent ||bc-layers are approximately oriented along the (−a+c)-direction. The preferred direction of the Fe^{2+} ion is more stable than its perpendicular direction by 7.5−8.7 k_BK per Fe (Table 3), and the strongest interlayer spin exchange $|J_5|$ is on the order of 0.9−1.7 k_BK (Table 2b). Therefore, in m-$NaFePO_4$, the spin order in the ||bc-layers set by the exchanges J_1, J_3, and J_4 and by the magnetic anisotropy cannot be destroyed by interlayer spin exchanges.

We now examine the preferred spin orientations of t-$NaFePO_4$ and m-$NaFePO_4$ from the viewpoint of their crystal-field split d-states. Using the coordinate system (x, y, z) for orbital, and (x', y', z') for spin, the SOC Hamiltonian $\hat{H}_{SO} = \lambda\hat{S}\cdot\hat{L}$ can be written as[22,24,25]

$$\hat{H}_{SO} \approx \hat{H}^0_{SO} = \lambda\hat{S}_{z'}\left(\hat{L}_z\cos\theta + \frac{1}{2}\hat{L}_+ e^{-i\varphi}\sin\theta + \frac{1}{2}\hat{L}_- e^{i\varphi}\sin\theta\right) \quad (4a)$$

$$\hat{H}_{SO} \approx \hat{H}^0_{SO} = \lambda\hat{S}_{z'}(\hat{L}_z\cos\theta + \hat{L}_x\sin\theta\cos\varphi + \hat{L}_y\sin\theta\sin\varphi) \quad (4b)$$

where the terms allowing interactions between up-spin and down-spin states (namely, the terms involving $\hat{S}_{+'}$ and $\hat{S}_{-'}$) are neglected. If an occupied down-spin d-state $\psi_{occ}\downarrow$ with energy e_{occ} interacts with an unoccupied down-spin d-state $\psi_{unocc}\downarrow$ with energy e_{unocc} via the matrix element $\langle\psi_{occ}|\hat{H}^0_{SO}|\psi_{unocc}\rangle$, the associated energy lowering ΔE_{SOC} is given by

$$\Delta E_{SOC} = -\frac{\left|\langle\psi_{occ}|\hat{H}^0_{SO}|\psi_{unocc}\rangle\right|^2}{|e_{occ} - e_{unocc}|} \quad (5)$$

where the matrix element $\langle\psi_{occ}|\hat{H}^0_{SO}|\psi_{unocc}\rangle$ depends on the spin orientation (i.e., the orientation of the z'-axis with respect to the (x, y, z) coordinate system. If the $\langle\psi_{occ}|\hat{H}^0_{SO}|\psi_{unocc}\rangle$ elements are comparable in magnitude, the most important interaction would be that between the highest occupied (HO) and the lowest unoccupied (LU) states.[9−13] Eq. 5 is also valid for the interactions of occupied up-spin d-states with unoccupied up-spin states. By convention, however, for magnetic ions with more than a half-filled d-shell, the HO and LU d-states typically occur within the down-spin (i.e., minority-spin) states. Eq. 4b reveals that the preferred spin orientation along the ||z-direction (θ = 0°, easy-axis anisotropy) requires a nonzero $\langle\psi_{occ}|\hat{L}_z|\psi_{unocc}\rangle$, that along the ||$x$-direction ($\theta$ = 90°, ϕ = 0°, easy-plane anisotropy) requires a nonzero $\langle\psi_{occ}|\hat{L}_x|\psi_{unocc}\rangle$, and that along the ||$y$-direction ($\theta$ = 90°, ϕ = 90°, easy-plane anisotropy) requires a nonzero $\langle\psi_{occ}|\hat{L}_y|\psi_{unocc}\rangle$.

The split d-states for a distorted FeO_6 octahedron of t-$NaFePO_4$ are shown in Figure 3a in terms of the projected density of states (PDOS) plots, and those for a distorted FeO_6 octahedron of m-$NaFePO_4$ are shown in Figure 3b. Here, the d-states are characterized by employing the local Cartesian coordinates presented in Figure 1d for t-$NaFePO_4$ and in Figure 2c for m-$NaFePO_4$. The HO and LU states of an FeO_6 octahedron in t-$NaFePO_4$ are described by $xz\downarrow$ and x^2-$y^2\downarrow$, respectively (Figure 3a). For these two states, $\langle xz|\hat{L}_x|x^2-y^2\rangle = 0$, $\langle xz|\hat{L}_y|x^2-y^2\rangle = -i$, and $\langle xz|\hat{L}_z|x^2-y^2\rangle = 0$.[25] This predicts that the preferred spin orientation is the y-axis, namely, the b-direction as observed for t-$NaFePO_4$.[3]

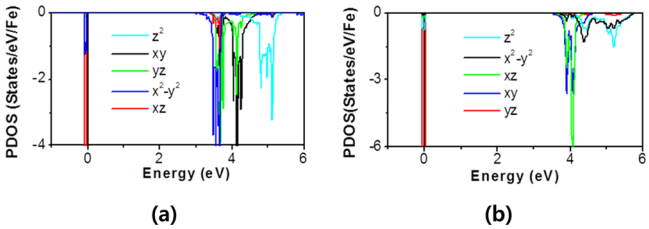

Figure 3. PDOS plots of the down-spin Fe d-states calculated for a selected FeO_6 octahedron from DFT+U calculations (with U_{eff} = 4 eV) of (a) t-$NaFePO_4$ (coordinates defined in Figure 1d) and (b) m-$NaFePO_4$ (coordinates defined in Figure 2c). The values of the PDOS are given in negative numbers to indicate that they are for the down-spin states.

The PDOS plots of m-$NaFePO_4$ in Figure 3b show that the HO d-state is given by $yz\downarrow$ and the LU d-state by both $xy\downarrow$ and $xz\downarrow$. The observed spin orientation of each FeO_6 octahedron in m-$NaFePO_4$ is the local x-direction, namely, along the short Fe−O_s bonds. However, $\langle yz|\hat{L}_x|xy\rangle = 0$ and $\langle yz|\hat{L}_x|xz\rangle = 0$,

DOI: 10.1021/acs.inorgchem.5b00577
Inorg. Chem. 2015, 54, 4966−4971

whereas $\langle yz \mid \hat{L}_y \mid xy\rangle = -i$ and $\langle yz \mid \hat{L}_z \mid xz\rangle = i$.[25] Thus, the HO−LU interactions predict that the preferred spin orientation is either the *y*- or *z*-axis direction, which disagrees with the experimental data.[3] However, we note that $yz\downarrow$ interacts with both $z^2\downarrow$ and $x^2\text{-}y^2\downarrow$ with $\langle yz \mid \hat{L}_x \mid z^2\rangle = -i\sqrt{3}$ and $\langle yz \mid \hat{L}_x \mid x^2 - y^2\rangle = -i$.[25] Note that the matrix element $\langle yz \mid \hat{L}_x \mid z^2\rangle$ is stronger than all of the other nonzero matrix elements involving $yz\downarrow$. As a result, the *x*-direction (i.e., Fe−O_s bond direction) becomes the preferred orientation.

Finally, we comment on a probable cause for the doubling of the *a*-axis length in the magnetic structure of m-$NaFePO_4$. As depicted in Figure 2d and e, the orthogonal spin arrangement between adjacent ∥*bc*-layers can be achieved regardless of whether the *a*-axis length is doubled (Figure 2d) or not (Figure 2e). We examine the energy difference between the two spin arrangements in terms of MDD interactions.[11,26,27] Given that two spins located at sites *i* and *j* are described by the distance r_{ij} with the unit vector $\vec{e}_{ij}$ along the distance, the MDD interaction is described by[11,26,27]

$$\left(\frac{g^2\mu_B^2}{a_0^3}\right)\left(\frac{a_0}{r_{ij}}\right)^3 [-3(\vec{S}_i\cdot\vec{e}_{ij})(\vec{S}_j\cdot\vec{e}_{ij}) + (\vec{S}_i\cdot\vec{S}_j)] \quad (6)$$

where a_0 is the Bohr radius (0.529177 Å), and $(g\mu_B)^2/(a_0)^3$ = 0.725 meV. We used the Ewald summation method[28−30] to sum the MDD interactions between various pairs of spin sites. Our MDD calculations show that the two ordered spin arrangements presented in Figure 2d and e are practically the same. Statistically, then, one-half of a given sample of m-$NaFePO_4$ would have the spin arrangement of Figure 2d and the remaining half would have the spin arrangement of Figure 2e. In NPD of m-$NaFePO_4$, the spin arrangement of Figure 2d should show a magnetic peak at midpoints between the Bragg peaks associated with the repeat distance *a*, but that of Figure 2e does not. The combined result of the two would be the presence of the magnetic peak, indicating the occurrence of *a*-axis length doubling.

4. CONCLUSION

In summary, the 3D AFM structure q_1 = (0, 0, 0) of t-$NaFePO_4$ is determined mainly by the spin exchanges J_1 and J_6. The exchange J_1 forms 2D AFM sheets parallel to the *bc*-plane, which are antiferromagnetically coupled along the *a*-direction by J_6. Other spin exchanges do not add much spin frustration to this 3D AFM lattice; thus, the frustration index is small ($f \approx$ 1.7). The Curie−Weiss temperature θ of m-$NaFePO_4$, estimated from the mean-field theory, is smaller than that of t-$NaFePO_4$ by a factor of ∼3.5, indicating that the experimental θ derived for m-$NaFePO_4$ from the linear portion of the $1/\chi$ vs *T* plot is overestimated in magnitude by a similar factor. In describing the 3D AFM structure q_2 = (1/2, 0, 1/2) of m-$NaFePO_4$, the spin exchanges in the ∥*bc*-layer need to be considered, which lead to the FM chains of J_1 that are antiferromagnetically coupled by J_4 along the *c*-direction, as well as the magnetic anisotropy of each Fe^{2+} ion, which orients the Fe^{2+} spin along the short Fe−O_s bonds. The interlayer exchanges exert no effect on the magnetic structure of each ∥*bc*-layer because the magnetic anisotropy of the Fe^{2+} ion is stronger than the strongest interlayer exchange. The doubling of the *a*-axis length suggested by the magnetic superstructure q_2 is caused most likely by the fact that the two ordered spin arrangements, presented in Figure 2d and e, are equally probable. It is satisfying to observe that the preferred orientations of the high-spin Fe^{2+} (d^6, S = 2) ions in the two polymorphs can be understood by perturbation theory using spin−orbit coupling as perturbation.

■ ASSOCIATED CONTENT

Supporting Information

Ordered spin states of t- and m-$NaFePO_4$, relative energies of the seven ordered spin state by DFT+U, and n1−n6 coefficients defining the total spin state exchange energies of the spin-ordered states. This material is available free of charge via the Internet at http://pubs.acs.org.

■ AUTHOR INFORMATION

Corresponding Authors

*E-mail: hjkoo@khu.ac.kr.

*E-mail: mike_whangbo@ncsu.edu.

Notes

The authors declare no competing financial interest.

■ ACKNOWLEDGMENTS

The research at KHU was supported by the Basic Science Research Program through the National Research Foundation of Korea (NRF) funded by the Ministry of Education, Science and Technology (2010-0021042), and the work at NCSU was funded by the computing resources of the NERSC Center and the HPC Center of NCSU.

■ REFERENCES

(1) Bridson, J. N.; Quinlan, S. E.; Tremaine, P. R. *Chem. Mater.* **1998**, *10*, 763−768.

(2) Moreau, P.; Guyomard, D.; Gaubicher, J.; Boucher, F. *Chem. Mater.* **2010**, *22*, 4126−4128.

(3) Avdeev, M.; Mohamed, Z.; Ling, C. D.; Lu, J.; Tamaru, M.; Yamada, A.; Barpanda, P. *Inorg. Chem.* **2013**, *52*, 8685−8693.

(4) Oh, S.-M.; Myung, S.-T.; Hassoun, J.; Scrosati, B.; Sun, Y.-K. *Electrochem. Commun.* **2012**, *22*, 149−152.

(5) Casas-Cabanas, M.; Roddatis, V.; Saurel, D.; Kubiak, P.; Carretero-González, J.; Palomares, V.; Serras, P.; Rojo, T. *J. Mater. Chem.* **2012**, *22*, 17421−17423.

(6) Ong, S. P.; Chevrier, V. L.; Hautier, G.; Jain, A.; Moore, C.; Kim, S.; Ma, X.; Ceder, G. *Energy Environ. Sci.* **2011**, *4*, 3680−3688.

(7) Greedan, J. E. *J. Mater. Chem.* **2011**, *11*, 37−53 and references cited therein.

(8) Smart, S. J. *Effective Field Theory of Magnetism*; Saunders: Philadelphia, PA, 1966.

(9) Xiang, H. J.; Wei, S.-H.; Whangbo, M.-H.; Da Silva, J. L. F. *Phys. Rev. Lett.* **2008**, *101*, 037209/4.

(10) Xiang, H. J.; Wei, S.-H.; Whangbo, M.-H. *Phys. Rev. Lett.* **2008**, *100*, 167207/4.

(11) Koo, H.-J.; Xiang, H. J.; Lee, C.; Whangbo, M.-H. *Inorg. Chem.* **2009**, *48*, 9051−9053.

(12) Ji, S.; Kan, E. J.; Whangbo, M.-H.; Kim, J.-H.; Qiu, Y.; Matsuda, M.; Yoshida, H.; Hiroi, Z.; Green, M. A.; Ziman, T.; Lee, S.-H. *Phys. Rev. B* **2010**, *81*, 094421/7.

(13) Liu, J.; Koo, H.-J.; Kremer, R. K.; Whangbo, M.-H. *J. Chem. Phys.* **2014**, *141*, 124113/7.

(14) Kresse, G.; Hafner, J. *Phys. Rev. B* **1993**, *47*, 558−561.

(15) Kresse, G.; Furthmüller, J. *Comput. Mater. Sci.* **1996**, *6*, 15−50.

(16) Kresse, G.; Furthmüller, J. *Phys. Rev. B* **1996**, *54*, 11169−11186.

(17) Perdew, J. P.; Burke, K.; Ernzerhof, M. *Phys. Rev. Lett.* **1996**, *77*, 3865−3868.

(18) Dudarev, S. L.; Botton, G. A.; Savrasov, S. Y.; Humphreys, C. J.; Sutton, A. P. *Phys. Rev. B* **1998**, *57*, 1505−1509.

(19) Dai, D.; Whangbo, M.-H. *J. Chem. Phys.* **2001**, *114*, 2887−2893.

(20) Dai, D.; Whangbo, M.-H. *J. Chem. Phys.* **2003**, *118*, 29−39.

DOI: 10.1021/acs.inorgchem.5b00577
Inorg. Chem. 2015, 54, 4966−4971

(21) Whangbo, M.-H.; Koo, H.-J.; Dai, D. *J. Solid State Chem.* **2003**, *176*, 417−481 and references cited therein.
(22) Xiang, H. J.; Lee, C.; Koo, H.-J.; Gong, X. G.; Whangbo, M.-H. *Dalton Trans.* **2013**, *42*, 823−853 and references cited thererin.
(23) Goodenough, J. B., *Magnetism and the Chemical Bond*, Interscience (Wiley): New York, 1963.
(24) Wang, X.; Wu, R.; Wang, D.-S.; Freeman, A. J. *Phys. Rev. B* **1996**, *54*, 61−64.
(25) Dai, D.; Xiang, H. J.; Whangbo, M.-H. *J. Comput. Chem.* **2008**, *29*, 2187−2209.
(26) Wu, F.; Kan, E. J.; Tian, C.; Whangbo, M.-H. *Inorg. Chem.* **2010**, *49*, 7545−7548.
(27) Tong, J.; Kremer, R. K.; Köhler, J.; Simon, I. A.; Lee, C.; Kan, E.; Whangbo, M.-H. *Z. Kristallogr.* **2010**, *225*, 498−503.
(28) Ewald, P. P. *Ann. Phys.* **1921**, *64*, 253−287.
(29) Darden, T.; York, D.; Pedersen, L. *J. Chem. Phys.* **1993**, *98*, 10089−10092.
(30) Wang, H.; Dommert, F.; Holm, C. *J. Chem. Phys.* **2010**, *133*, 034117/12.

DOI: 10.1021/acs.inorgchem.5b00577
Inorg. Chem. 2015, 54, 4966−4971